Threshold Barrier of Carbon Nanotube Growth

Qinghong Yuan,[1] Hong Hu,[1] and Feng Ding[1,2,*]

[1]*Institute of Textile and Clothing, Hong Kong Polytechnic University, Kowloon, Hong Kong, People's Republic of China*
[2]*National Laboratory of Infrared Physics, Shanghai Institute of Technical Physics,*
Chinese Academy of Science, Shanghai 200083, People's Republic of China

A previously overlooked step of carbon nanotube (CNT) growth, incorporating C atoms into the CNT wall through the CNT-catalyst interface, is studied by density functional theory calculations. A significant barrier for incorporating C atoms into the CNT wall (~ 2 eV for most used catalysts, Fe, Co, and Ni) is revealed and the incorporation can be the threshold step of CNT growth in most experiments. In addition, the temperature dependent CNT growth rate is calculated and our calculation demonstrates that growing 0.1–1 m long CNTs in 1 h is theoretically possible.

Incorporating carbon atoms that are dissociated from feedstock gas into a carbon nanotube (CNT) wall in a repeatable manner is crucial in CNT growth. A deep understanding of the process may lead to experimental design for controlled CNT synthesis. A repeatable cycle of transforming two C atoms from feedstock into one 6-membered-ring (6MR) on the growth front (or the open end) of a CNT, which is attached to a catalyst particle surface, can be divided into three sequential steps: (i) catalytic decomposition of feedstock molecules, (ii) diffusion of the released C atoms to a nearby site of the CNT open end, and (iii) the direct incorporation of the C atoms into the tube wall [1–4]. Among the three steps, which one is the threshold step in CNT growth has been argued for a long time. Hofmann and co-workers have shown that step (ii), the C atom diffusion through catalyst surface, is the threshold step of multiwalled CNTs' (MWNTs) growth from Fe catalyst [4]. On the other hand, Mora *et al.* have shown that the low temperature growth of single walled CNTs (SWNTs) is feedstock decomposition limited, or step (i) is the threshold [1]. Step (iii), directly incorporating C atoms into the CNT wall, has never been considered as the threshold step because of the high activity of the CNT open end and the exothermic reaction of incorporating C atoms into a tube wall.

Recently, mimicking the role of screw dislocation in crystal growth, Ding and co-workers applied the traditional concept of screw dislocation in SWNT growth and revealed that the growth rate of a SWNT is proportional to the number of active sites [i.e., armchair (AC) sites] on the tube-catalyst interface [5]. It is rather surprising that such a simple theory fits most known experimental results very well [5]. Here we address the notion that a precondition for the validity of the screw dislocation theory is that the SWNT growth must be limited by the direct incorporation of C atoms into a SWNT wall or step (iii) is the threshold step of SWNT growth. Such a precondition is logically

easily understood If (i), the feedstock decomposition, or (ii), the C diffusion on catalyst surface, is the threshold step, the SWNT growth rate should be proportional to the number of decomposed C atoms or the number of C atoms that reach the SWNT-catalyst interface instead of the number of active AC sites. Therefore, the good fitting between the screw dislocation theory and most known experimental results implies that incorporating C atoms into a SWNT wall is the threshold step in most experiments.

The CNT growth rate, which is limited by a threshold barrier, is a crucial parameter in CNT synthesis. The recorded CNT growth rate, $R = 100$ μm/s, was reported by Wen *et al.* in a Fe catalyzed CH_4-H_2O chemical vapor deposition (CVD) experiment at the temperature of $T = 1273$ K [6]. Such a high growth rate means that incorporating two C atoms to an AC site through the CNT-catalyst interface must occur in a very short time scale of $\tau = 10^{-6}$ s (see [7]). According to the transition state theory (TST), incorporating two C atoms in such a short period implies that the threshold barrier of CNT growth must be lower than

$$E_0^* < kT \ln[\tau(kT/h)] = 1.88 \text{ eV}, \qquad (1)$$

where k and h are Boltzmann and Plank constants, respectively. This anticipated barrier is in agreement with previously reported ones: 1.5–2.2 eV in CNT thermal CVD growth [8–11]. Does the barrier, E_0^*, correspond to direct incorporation of C atoms into a tube wall? Can such a barrier be further reduced by guided catalyst design, e.g., using alloy catalysts or recently discovered unconventional catalysts (Au, Cu, Pt, etc.) [12,13] instead of Fe in experiments? Answering these questions would achieve a deep insight into the CNT growth mechanism beyond the initial nucleation stage, which still remains a mystery after 2 decades of extensive exploration [3,5,14–24]. Additionally, it may lead to appropriate catalyst design for ultrafast CNT growth or diameter- and/or chirality-selected SWNT growth.

In this Letter, motivated by the precondition of applying screw dislocation theory in CNT growth and the ultrafast recorded CNT growth rate, we calculated the barrier of incorporating C atoms into a SWNT wall through the SWNT-catalyst interface. Our calculations demonstrate that the overall barriers of incorporating two C atoms into a SWNT wall are 1.85, 2.28, 2.27 eV for catalysts Fe, Co, and Ni, respectively. Such barriers are notably higher than either the known C diffusion barriers on metal surfaces (< 1.0 eV) [3,4,25–28] or the C feedstock decomposition barriers (< 1.5 eV) [4,29–32]. We therefore conclude that the direct incorporation of C atoms into a SWNT wall is the threshold step in SWNT growth. In addition, the calculated temperature dependent upper limit of CNT growth rate is in excellent agreement with broadly reported experimental data and shows that growing 10–100 cm long SWNTs in less than 1 h is theoretically possible.

To mimic many experimental observations [3,5,25,33–35], as shown in Figs. 1(a) and 1(b), a graphene edge attached to a metal step is used to model a fraction of the CNT-catalyst interface, and the generalized gradient approximation with Perdew-Burke-Ernzerhof functional [36] was used to calculate the barriers of incorporating C atoms into a CNT wall (for details see modeling and methods of calculation in [37]). Here only an armchair edge is considered because of the high nucleation barrier and the negligible growth rate at the zigzag edge [5]. A repeatable cycle of CNT growth includes incorporation of two C atoms into the CNT wall (as explained in the caption of Fig. 1).

The process of incorporating the first C atom into a SWNT wall attached to a step of the Ni(111) surface is shown in Fig. 1(c). Once the C atom reaches a site near the step, a slight lattice distortion leads to formation of the C atom located at the center of four Ni atoms [the initial state in Fig. 1(c)]. The transition state in Fig. 1(c) shows the lowest path for the C atom to reach the AC site, diffusion through the subsurface. Another high energy diffusion path, surface diffusion, is shown in Fig. S1 of [37]. The barrier of subsurface diffusion, 1.02 eV, is lower than that of surface diffusion, 1.27 eV. A metal stabilized hexagon structure [the final state in Fig. 1(c)] is formed after the incorporation of the first C atom. On a Ni(111) surface, the incorporation of the first C atom from the step edge is highly exothermic with a notable energy release of 0.9 eV. This is attributed to the high formation energy of the C monomer near the Ni(111) step edge, which is 0.97 eV/atom relative to graphene.

The incorporation of the second C atom leads to the removal and etching of one Ni atom simultaneously
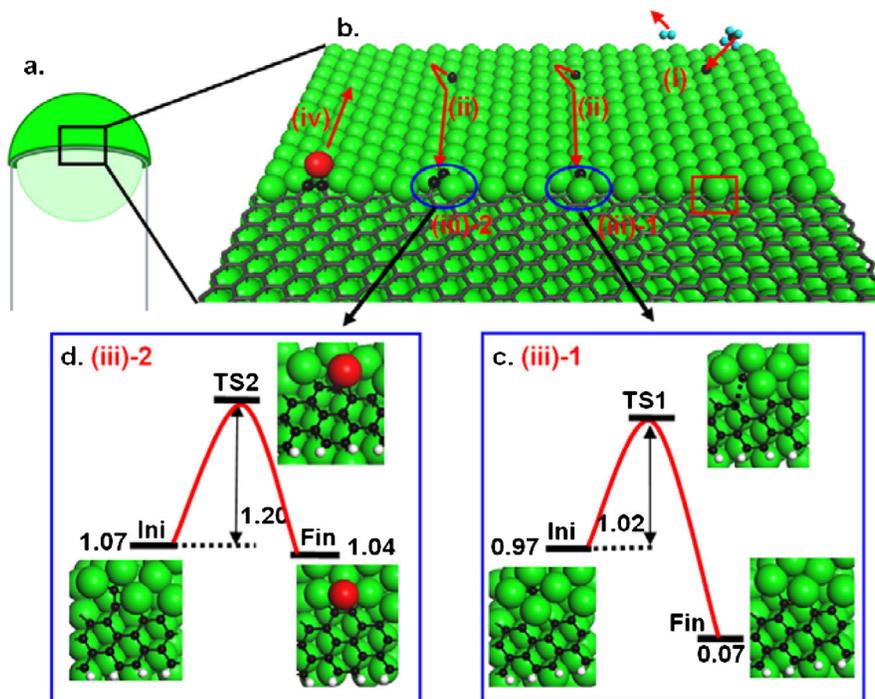

FIG. 1 (color online). (a) The SWNT-metal catalyst particle interface, where the circular tube open end is attached to a circular metal step edge on the catalyst particle. (b) A fraction of the SWNT-catalyst step interface is modeled by an interface of graphene-stepped metal surface [represented by the Ni(111) surface here]. A repeatable cycle of incorporating two C atoms into a new 6-membered-ring (6MR) on a CNT AC site involves 4 serial steps: (i) the decomposition of C feedstock molecules on catalyst surface; (ii) decomposed C atoms diffuse to a AC site; (iii)-1 and (iii)-2 the direct incorporation of the first and second C atoms into the AC site to form a new 6MR [the details of (iii)-1 and (iii)-2 shown in (c) and (d)]; (iv) the etched metal atom diffuse away, leading to a reconstruction of the catalyst.

because there is not enough space to accommodate two C and one Ni atoms. On a Ni(111) surface, a very small barrier is required to form a C-C bond between the second and the first added C atoms (see Fig. S4 in [37]), but overcoming a significant barrier is required to form a new hexagon on the tube end and simultaneously knock one metal atom away. As shown in Fig. 1(d), the activation barrier of anchoring the second C atom is 1.20 eV.

Combining the two sequential steps together, we can get the energy profile of a repeatable CNT growth cycle on a Ni(111) surface as presented in Fig. 2. It can be clearly seen that the overall barrier of the multistep reaction is the energy of the transition state of the second C insertion, that is, 2.27 eV. The last step, diffusion of Ni and the reconstruction of the catalyst, will lead the system to restore its original state [33], and thus the energy change of such a repeatable growth process is zero as the energy of graphene is used as the reference.

In the energy profile, we have neglected the barriers of C feedstock decomposition, C and Ni atom diffusions on the Ni(111) surface. These barriers are involved in the 1st and 2nd C decomposition, diffusion, metal diffusion, and catalyst reconstruction (represented by dashed lines in Fig. 2). As discussed before, these barriers are notably small and thus it is reasonable to neglect these details.

Similar to CNT growth on a Ni(111) surface, the calculated barriers for the first and second C addition into the CNT wall through the stepped Co(111) surface are 1.21 and 1.57 eV, and barriers through the stepped Fe(111) surface are 1.47 and 1.64 eV, respectively (details are shown in Figs. S2, S3, S5, and S6 in [37]).

The energy profiles of C insertion into the CNT wall on Co(111) and Fe(111) surfaces are shown in Fig. S7 in [37]. Similarly, the barriers are energies of transition states in anchoring the second C into the tube wall (2.28 and 1.85 eV, respectively). Compared with Ni and Co, Fe has the highest affinity with C atoms and thus the adsorbed C atom on the Fe surface has a low formation energy, which leads to a significant drop of the overall barrier. It

is important to note that, depending on the growth condition, an Fe catalyst may have a different crystalline structure or facets of different orientations, for example, fcc-Fe(100), fcc-Fe(110), bcc-Fe(100), and bcc-Fe(110). Further calculations showed that all these facets of Fe have higher affiliation to an adsorbed C atom [37] than Co and Ni. Among these three metals, the threshold barrier on Fe is the lowest, indicating its highest catalytic activity in CNT growth. It is important to note that, experimentally, Fe is the most used optimum catalyst in CNT synthesis, e.g., in supergrowth of CNT carpets and the CNT ultrafast growth through the kite mechanism [5,6,38,39].

Taking the energy of C in graphene as the reference, the overall barriers of incorporating two C atoms into a 6MR in a CNT wall through Ni, Co, and Fe surfaces are $G_0^* = 2.27$, 2.28, and 1.85 eV, respectively. However, the CNT cannot grow at such a condition because of the lack of driving force; i.e., the final and the initial states have exactly the same energy. In real CNT growth experiments, active C feedstock whose energy is higher than that of CNT is used. Denoting the chemical potential difference between a C atom in a CNT wall and in feedstock as $\Delta\mu$, the free energy of the initial state (i.e., the energy of two C atoms in feedstock) G_{Ini} rises to $2\Delta\mu$ and the overall barrier (Fig. 2) becomes

$$G^* = G_0^* - 2\Delta\mu. \qquad (2)$$

Now through the above calculations and analysis, the recorded ultrafast CNT growth rate can be easily understood. As estimated in the introduction, the recorded CNT growth rate, ~ 100 μm/s, requires a small threshold barrier of 1.88 eV or less. The calculated threshold barrier for CNT growth on Fe, $G^* = 1.85$ eV $- 2\Delta\mu$, fits the estimation perfectly. Furthermore, Eq. (2) also implies that the CNT growth rate might be further improved by using more active feedstock with larger $\Delta\mu$.

To calculate the CNT growth rate at a given $\Delta\mu$ and temperature T, the reverse process, decomposition of CNT, has to be considered as well. From energy profiles shown in
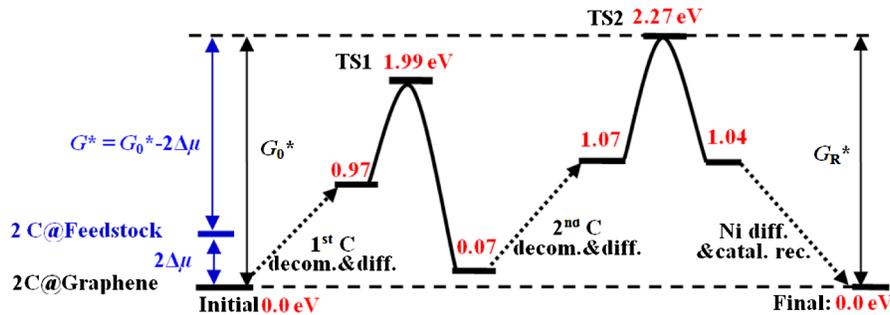

FIG. 2 (color online).   Energy profile for incorporating two C atoms into graphene on Ni(111) surface serially. A full cycle has zero energy change and the overall barrier G_0^* equals the barrier of a reverse procedure G_R^* when C in graphene is treated as initial feedstock. Using active C feedstock reduces the barrier to $G_0^* - 2\Delta\mu$, where $\Delta\mu$ is the chemical potential difference between a C in graphene and in feedstock. The details of feedstock decomposition, C diffusion, and metal diffusion are ignored and shown by dashed lines. In the figure, "decom.&diff." stands for decomposition and diffusion and "diff.&catal. rec." stands for diffusion and catalyst reconstruction.

Fig. 2 and in Fig. S7 in [37], it is easy to figure out that the overall energy barrier of the reverse process is G_0^*, which is independent of the feedstock type. So, by applying the TST, the reaction constants of CNT growth K^+ and CNT decomposition K^- can be written as

$$K^+ = (kT/h)\exp[-\beta(G_0^* - 2\Delta\mu)], \quad (3a)$$

$$K^- = (kT/h)\exp[-\beta G_0^*], \quad (3b)$$

where $\beta = 1/kT$. With sufficiently fast C feedstock decomposition and C diffusion, the growth rate of a (n, m) SWNT may reach its upper limit:

$$R_U(n, m) \sim m(b/D)(K^+ - K^-) \times 0.1 \text{ nm/s}$$
$$= \sin(\theta)(K^+ - K^-) \times 0.1 \text{ nm/s}, \quad (4)$$

where m is the number of active AC sites on the tube end, $b = 0.246$ nm, D is the diameter of the tube, and θ is the tube chiral angle. The factor 0.1 nm/s was added because inserting a full AC C ring onto a CNT results in a net tube elongation of $\sim$0.1 nm. Introducing Eq. (3) into Eq. (4), the upper limit of the CNT growth rate can be rewritten as

$$R_U(\theta) \sim 0.1\sin(\theta)(kT/h)\exp(-\beta E^*)$$
$$\times [\exp(2\beta\Delta\mu) - 1] \text{ nm/s} = 2\sin(\theta)R_{\text{UAC}}, \quad (5)$$

where $R_{\text{UAC}} = 0.05(kT/h)\exp(-\beta E^*)[\exp(2\beta\Delta\mu) - 1]$ nm/s is the upper limit of the armchair CNT's growth rate. Figure 3 shows R_{UAC} as a function of temperature and $\Delta\mu$, using Fe, Co, and Ni as catalysts, respectively. Considering a medium driving force, $\Delta\mu = 0.1$ eV, the upper limit of CNT growth rate using Fe as catalyst reaches 10^4–10^6 nm/s or 0.01–1 mm/s in the temperature range from 1100 to 1300 K. This is in agreement with the recorded CNT growth rate (the scattered symbols in Fig. 3). In real CNT growth conditions, beyond the
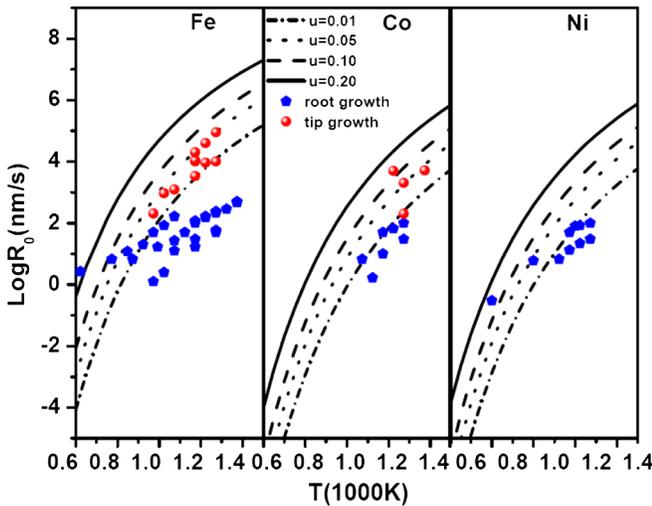

FIG. 3 (color online).   CNT growth rate on Ni, Co, Fe surfaces versus growth temperature at different $\Delta\mu$ (in eV).

threshold barrier, there are many others parameters (e.g., type, partial pressure of C feedstock, addition of hydrogen or water, substrate materials, etc.) that may change the rate of CNT growth. To compare with experimental results, more than 50 experimentally measured CNT growth rates at very different temperatures (for both tip growth, also called "kite mechanism," and root growth, the supergrowth of CNT carpet) are plotted in Fig. 3 (for details see Table S1 in [37]). We find the following.

(i) These experimental growth rates fit the theoretical curves well in a very large growth rate range from 10^1 to 10^5 nm/s and a wide temperature range from 700 to 1300 K.

(ii) The CNT growth rate in "kite growth" is normally several orders of magnitude faster than that of CNT carpet growth. This implies that CNT carpet growth is not limited by the threshold barrier of incorporating C atoms into a CNT wall. Instead, carpet growth may be limited by the low carbon feedstock deposition rate to the catalyst surface because feedstock molecules have to diffuse through the densely packed long CNT forest to reach the catalyst at the CNT foot. In such a case, the relationship $R \sim \sin(\theta)$ may not be maintained. In the CNT carpet growth, all CNTs are entangled together and thus they have to grow at the same rate, which is notably smaller than the upper limit rate.

(iii) Using Fe as the catalyst in kite growth leads to a larger growth rate than using Co or Ni because of its lowest barrier, G^*. That is in agreement with experimental observation. For example, the recorded CNT kite growth using Co is about 1 order of magnitude slower than that of using Fe.

It is known that the kite mechanism can only be used to grow a very limited amount of CNTs which are high quality and every tube can be extremely long (up to 10 cm) [6]. In contrast, the supergrowth of a CNT carpet can be used to synthesize CNTs in large quantity, but the tube quality is relatively low. Their comparison (Fig. 3) reveals that the significant difference originated from their different threshold steps: the former is limited by the incorporation of C atoms into the CNT wall and the latter is limited by the C feedstock deposition rate to the catalyst. This implies that by increasing feedstock deposition rate in CNT carpet growth (e.g., if CNT carpet growth can be achieved by tip growth), we are probably able to synthesize ultralong carpet CNTs, e.g., $\sim$10–100 cm or longer in a reasonable experimental time, e.g., 1 hr.

In conclusion, we have performed a comprehensive study of incorporating C atoms into a CNT wall. The calculated high overall barriers (2.27, 2.28, and 1.85 eV for Ni, Co, and Fe, respectively) indicate that incorporating a C atom into a CNT wall can be the threshold step of CNT growth. We should, however, point out that the overall growth rate can remain proportional to the number of active sites or kinks (and therefore the chiral angle) even if

the threshold is the diffusion [40]. In addition, the analysis of the upper limit of the CNT growth rate confirms that Fe is the best catalyst for fast CNT growth because of its low threshold barrier. The study also reveals the potential of growing ultralong CNTs in a short period. For example, CNT growth at the rate of 10–100 cm/h is theoretically possible. The deep insight into the CNT growth mechanism presented in this study will certainly benefit the experimental design of controlled CNT growth.

---

*Corresponding author.
tcfding@inet.polyu.edu.hk

[1] E. Mora *et al.*, J. Am. Chem. Soc. **130**, 11840 (2008).
[2] F. Ding, A. Rosen, and K. Bolton, Chem. Phys. Lett. **393**, 309 (2004).
[3] F. Abild-Pedersen *et al.*, Phys. Rev. B **73**, 115419 (2006).
[4] S. Hofmann *et al.*, Phys. Rev. Lett. **95**, 036101 (2005).
[5] F. Ding, A. R. Harutyunyan, and B. I. Yakobson, Proc. Natl. Acad. Sci. U.S.A. **106**, 2506 (2009).
[6] Q. Wen *et al.*, Chem. Mater. **22**, 1294 (2010).
[7] Inserting a ring of C atoms on a SWNT open end leads to $\Delta L \sim 0.1$ nm or 10^{-4} μm elongation of the tube and thus incorporating two C atoms to an AC site through the CNT-catalyst interface must occur in a time scale of $\tau = \Delta L/R \sim 10^{-6}$ s.
[8] X. F. Feng *et al.*, J. Phys. Chem. C **113**, 9623 (2009).
[9] L. B. Zhu *et al.*, Carbon **45**, 344 (2007).
[10] D. B. Geohegan *et al.*, Appl. Phys. Lett. **83**, 1851 (2003).
[11] Y. T. Lee *et al.*, Chem. Phys. Lett. **372**, 853 (2003).
[12] S. M. Huang *et al.*, J. Am. Chem. Soc. **131**, 2094 (2009).
[13] D. Takagi *et al.*, Nano Lett. **6**, 2642 (2006).
[14] J. Gavillet *et al.*, Phys. Rev. Lett. **87**, 275504 (2001).
[15] F. Ding *et al.*, Nano Lett. **8**, 463 (2008).
[16] F. Ding, A. Rosen, and K. Bolton, J. Chem. Phys. **121**, 2775 (2004).
[17] F. Ding, K. Bolton, and A. Rosen, J. Phys. Chem. B **108**, 17 369 (2004).
[18] M. Kumar and Y. Ando, J. Nanosci. Nanotechnol. **10**, 3739 (2010).
[19] A. J. Page *et al.*, Acc. Chem. Res. **43**, 1375 (2010).
[20] J. Zhao, A. Martinez-Limia, and P. B. Balbuena, Nanotechnology **16**, S575 (2005).
[21] A. Borjesson *et al.*, Nano Lett. **9**, 1117 (2009).
[22] E. C. Neyts *et al.*, ACS Nano **4**, 6665 (2010).
[23] Y. Shibuta and S. Maruyama, Chem. Phys. Lett. **382**, 381 (2003).
[24] J. Y. Raty, F. Gygi, and G. Galli, Phys. Rev. Lett. **95**, 096103 (2005).
[25] S. Helveg *et al.*, Nature (London) **427**, 426 (2004).
[26] J. Robertson *et al.*, J. Nanosci. Nanotechnol. **8**, 6105 (2008).
[27] M. Ikeda, T. Yamasaki, and C. Kaneta, J. Phys. Condens. Matter **22**, 384214 (2010).
[28] The barrier for C diffusion is ~ 0.3–0.9 eV [3,4,25–27] according to different feedstock and catalytic metal surfaces. The barrier for C diffusion on a Ni surface is 0.3–0.7 eV [3,4,25,26] and on an Fe surface is 0.91 eV [27].
[29] S. Nave and B. Jackson, Phys. Rev. Lett. **98**, 173003 (2007).
[30] F. Abild-Pedersen *et al.*, Surf. Sci. **590**, 127 (2005).
[31] D. C. Sorescu, Phys. Rev. B **73**, 155420 (2006).
[32] The reported barrier for feedstock decomposition is ~ 0.85–1.3 eV [4,29–31] according to different feedstock and catalytic metal surfaces. The barriers for CH_4 and C_2H_2 decomposition on Ni surfaces are ~ 1.0 and ~ 1.3 eV, respectively [4,28], and barriers for CH_4 and C_2H_2 decomposition on Fe surfaces are 0.85 [31] and 0.96 eV [29], respectively.
[33] M. Moseler *et al.*, ACS Nano **4**, 7587 (2010).
[34] J. A. Rodriguez-Manzo *et al.*, Small **5**, 2710 (2009).
[35] S. Hofmann *et al.*, Nano Lett. **7**, 602 (2007).
[36] J. P. Perdew, K. Burke, and M. Ernzerhof, Phys. Rev. Lett. **77**, 3865 (1996).
[37] See Supplemental Material at http://link.aps.org/supplemental/10.1103/PhysRevLett.107.156101 for computational details, reactions of the first and second C addition on Ni(111), Co(111), and Fe(111) surfaces, energy profiles of C addition on Co(111) and Fe(111) surfaces, experimentally measured CNT growth rates, and C affinity on different surfaces of Fe, Co, and Ni crystals.
[38] L. X. Zheng *et al.*, Nature Mater. **3**, 673 (2004).
[39] S. J. Kang *et al.*, Nature Nanotech. **2**, 230 (2007).
[40] S. I. Temkin and B. I. Yakobson, J. Phys. Chem. **88**, 2679 (1984).